

Extreme events and power-law distributions from nonlinear quantum dissipation

Wai-Keong Mok¹

¹*Institute for Quantum Information and Matter,
California Institute of Technology, Pasadena, CA 91125, USA*

Power-law probability distributions are widely used to model extreme statistical events in complex systems, with applications to a vast array of natural phenomena ranging from earthquakes to stock market crashes to pandemics. We propose the emergence of power-law distributions as a generic feature of quantum systems with strong nonlinear dissipation. We introduce a prototypical family of quantum dynamical systems with nonlinear dissipation, and prove analytically the emergence of power-law tails in the steady state probability distribution for energy. The power law physically originates from the amplification of quantum noise, where the scale of the microscopic fluctuations grows with the energy of the system. Our model predicts a power-law regime with infinite mean energy, which manifests as extreme events and divergences in the measurement statistics. Furthermore, we provide numerical evidence of power-law distributions for a general class of nonlinear dynamics known as quantum Liénard systems. This phenomenon can be potentially harnessed to develop extreme photon sources for novel applications in light-matter interaction and sensing.

Introduction.— The natural occurrence of power-law probability distributions underpin many fascinating statistical phenomena in complex systems across vast domains such as physics, biology, geology, economics and social science [1–4]. Power-law distributions are often associated with the presence of extreme or ‘black swan’ events, which are statistical events that occur with low frequency but yet have enormous impact [5, 6]. This is sometimes stated in various contexts as the Pareto principle: a majority of the observed effects arise from a minority of the causes. Extreme events are abound in nature, with well-known examples including earthquakes [7], rogue ocean waves [8], solar flares [9], stock market crashes [10] and pandemics [11].

Often, extreme events are observed as emergent phenomena in large-scale systems, and statistical models are constructed to explain the empirical data *a posteriori*. Here, we show that such a phenomenon can emerge dynamically in one of the most fundamental stochastic system in nature — a single dissipative quantum system. To this end, we construct a prototypical model of a quantum dynamical system with nonlinear dissipation, and prove analytically that the steady state probability distribution for the energy exhibits a power-law tail. If we regard the system physically as a quantum particle trapped in a potential well, this phenomenon manifests as a power-law decay in the position and momentum distribution of the quantum particle [12, 13].

The physical origin of the power-law distribution in our model can be attributed to quantum noise [14]. The phenomenon stems from the intimate connection between microscopic fluctuations and dissipation in quantum mechanics, and traces back to Heisenberg’s uncertainty principle. From the perspective of open quantum systems, the microscopic interactions between the system and the external bath, which is responsible for the dissipation, must inject noise into the system [14–16]. Furthermore, the form of this quantum noise is highly dependent on the type of dissipation. For nonlinear dissipation, this noise is typically multiplicative, which means the noise

is coupled to the quantum state of the system [17, 18]. In our model, the coupling induces a self-amplification of the noise, in which the scale of the fluctuations grow with the excitation of the system. The amplified fluctuations at large excitation are only weakly suppressed by the dissipation, and the net result is a power-law distribution.

Our model predicts a regime where the power-law tail vanishes so slowly such that the quantum state, while normalizable, contains an infinite number of excitation quanta on average. Moreover, the distribution for the excitation number is highly skewed towards low excitation. This gives rise to extreme events in which the system, when measured in the excitation number basis, produces highly excited states containing orders of magnitude more excitation quanta than the typically measured values. This regime of the power law was previously observed experimentally in a different nonlinear quantum optical setup, which works by amplifying the vacuum fluctuations [19]. In that experiment, extreme emission events containing $\sim 10^6$ photons in a single pulse were observed.

Applying our model to the context of quantum optics, where the excitations are now photons, our analytical results show that the system can exhibit an extreme case of photon superbunching whereby the emitted photons are significantly more correlated in time as compared to thermal light sources [20]. The intensity correlation function (at zero delay) in this case can be made arbitrarily high, due to the strong fluctuations in the electromagnetic field. We establish quantitative predictions for various physical quantities, which can serve as experimental signatures of the power-law distribution.

Finally, we propose that the emergence of a power-law tail is a generic feature of quantum systems with strong nonlinear dissipation. To support this claim, we study a wide range of nonlinear dissipative models proposed in Refs. [21, 22], which are quantum analogs of the Liénard system. The Liénard system is a general class of nonlinear dynamical models containing many paradigmatic examples such as the van der Pol, Rayleigh, and Duffing

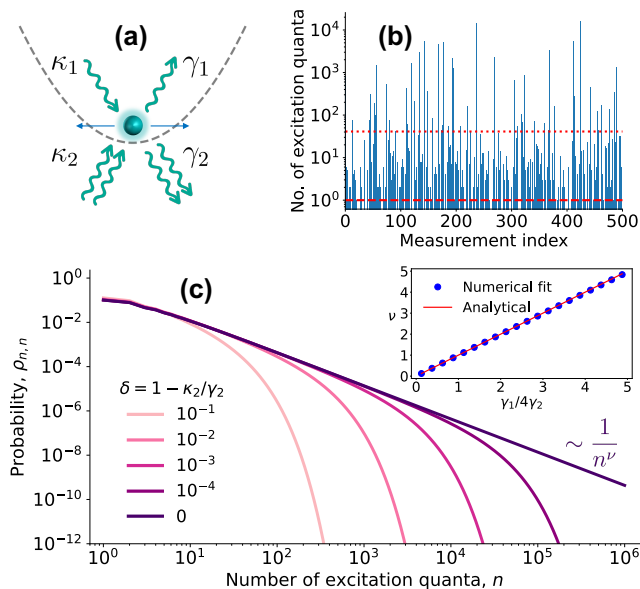


FIG. 1. (a) A quantum particle trapped in a one-dimensional harmonic potential interacts with M independent baths ($M = 2$ depicted). The particle exchanges m excitation quanta with the m -th bath ($m = 1, \dots, M$), at a dissipation rate of γ_m and pumping rate of κ_m . (b) Simulated measurement for the number of excitation quanta n on the steady state of Eq. (1) with $M = 2$ and 500 measurement samples. The dashed line indicates the median count $n = 1$, and the dotted line indicates the 90th percentile count $n \approx 41.1$. Extreme events reaching $n \approx 16000$ are observed. Parameters are $\{\gamma_1, \kappa_1, \gamma_2, \kappa_2\} = \{6, 0, 1, 1\}$. (c) The probability distribution $\rho_{n,n}$ for n exhibits a power-law tail $\sim n^{-\nu}$ at the critical point $\kappa_2 = \gamma_2$, plotted for $\gamma_1/\gamma_2 = 6$ and $\kappa_1/\gamma_2 = 0$. The inset shows the power-law exponent ν against $\gamma_1/4\gamma_2$. The data points are obtained by numerically fitting with a power law, which agrees excellently with the analytical result (3), $\nu = \gamma_1/4\gamma_2$. Away from the critical point, the probability distribution follows a power law up to an exponential cutoff at $n \approx 2/\delta$.

oscillators [23]. We show numerically that, for strong dissipation and typical parameters, the steady state density matrix in the excitation number basis exhibits a power-law tail in the diagonal elements (which correspond to the probability distribution), and also in the off-diagonal elements (which correspond to the quantum coherences) with the same scaling behavior.

M-boson model. — Consider the system to be a quantum harmonic oscillator, with a characteristic energy scale $\hbar\omega_0$. The system interacts with M independent baths, by exchanging m excitation quanta with the m -th bath ($m = 1, \dots, M$), at dissipation and pumping rates denoted by γ_m and κ_m respectively [see Fig. 1(a)]. For a bath at thermal equilibrium, the ratio $0 \leq \kappa_m/\gamma_m \leq 1$ is determined by the temperature of the bath, where the lower and upper limits correspond to zero and infinite temperatures respectively. Under the Born-Markov approximation, the quantum dynamics of the system can

be modelled by the Lindblad master equation [14–16]

$$\dot{\rho} = -i[\omega_0 \hat{a}^\dagger \hat{a}, \rho] + \sum_{m=1}^M (\gamma_m \mathcal{D}[\hat{a}^m] \rho + \kappa_m \mathcal{D}[\hat{a}^{\dagger m}] \rho) \quad (1)$$

for the density matrix ρ of the system, where $\mathcal{D}[\hat{c}]\rho \equiv \hat{c}\rho\hat{c}^\dagger - (\hat{c}^\dagger\hat{c}\rho + \rho\hat{c}^\dagger\hat{c})/2$ is the dissipator. The annihilation and creation operators \hat{a} and \hat{a}^\dagger for the system excitation satisfy the bosonic commutation relation $[\hat{a}, \hat{a}^\dagger] = 1$. The model can physically describe, for instance, photonic excitations (in optical or microwave cavities) or phononic excitations (in a trapped ion or nanomechanical resonator). In Eq. (1), the bath degrees of freedom are traced out, and the effects of the microscopic system-bath interactions are captured by the dissipator terms. We shall refer to Eq. (1) as the *M-boson model*. The case of $M = 1$ reduces to the well-known example of a damped harmonic oscillator [14–16], while the $M = 2$ case was previously studied in the context of quantum limit cycles and synchronization [18, 24–27]. We remark that γ_2 dissipation term was implemented experimentally on superconducting circuits using dissipation engineering, to stabilize Schrödinger cat states for bosonic error correction [28, 29]. A similar setup can be used to implement the κ_2 pumping term.

Since Eq. (1) is rotationally symmetric (i.e., invariant under the $U(1)$ transformation $\hat{a} \rightarrow e^{i\phi}\hat{a}$), the steady state density matrix is diagonal in the excitation number basis $\{|n\rangle\}$ and independent of ω_0 . In this basis, Eq. (1) simplifies to

$$\begin{aligned} \dot{\rho}_{n,n} = & \sum_{m=1}^M \gamma_m \left[\rho_{n+m,n+m} \prod_{j=1}^m (n+j) - \rho_{n,n} \prod_{j=0}^{m-1} (n-j) \right] \\ & + \sum_{m=1}^M \kappa_m \left[\rho_{n-m,n-m} \prod_{j=0}^{m-1} (n-j) - \rho_{n,n} \prod_{j=1}^m (n+j) \right], \end{aligned} \quad (2)$$

with the coherences (off-diagonal elements of ρ) decoupled from the probability distribution $\rho_{n,n}$. Solving for the steady state $\dot{\rho}_{n,n} = 0$ yields the truncated power-law tail

$$\rho_{n,n} \propto \frac{e^{-n\delta/M}}{n^\nu}, \quad \nu = \frac{M-1}{M^2} \frac{\gamma_{M-1} - \kappa_{M-1}}{\gamma_M} \quad (3)$$

for large n , small $\delta \equiv \gamma_M/\kappa_M - 1 \geq 0$, and any $M \geq 2$, see Supplementary Materials (SM) for details [30]. The power-law tail is exact at the critical point $\delta = 0$, which can be physically interpreted as fixing the M -th bath at infinite temperature. The power-law behavior is almost entirely controlled by the leading order processes involving M and $M-1$ bosons, which is intuitive since these processes dominate the dynamics at large n . By tuning the rates γ_{M-1} and κ_{M-1} (for example, by adjusting the temperature of the $(M-1)$ -th bath), the power-law exponent ν can vary between 0 and ∞ . The regime $\nu \leq 2$ is

particularly interesting, where the mean excitation number is infinite at criticality. As shown in Fig. 1(b), this can give rise to extreme events where the measured excitation numbers are orders of magnitude higher than typical values, following the power-law behavior as shown in Fig. 1(c). More generally, the k -th moment of the number distribution $\rho_{n,n}$ is infinite or undefined if $\nu \leq k + 1$. Away from the critical point, Eq. (3) predicts an exponential cutoff at $n \sim M/\delta$. For $\delta \ll 1$, the power-law behavior holds for a large range of n . This suggests that the dramatic effects of the power-law tail, such as extreme events, can be observed close to the critical point.

The power-law behavior at criticality might appear surprising, since the M -boson exchanges in and out of the system occur at precisely the same rate $\gamma_M = \kappa_M$. The emergence of the power law can be understood by examining the quantum fluctuations. Taking the white-noise limit of the bath, the master equation (1) yields, in the Heisenberg picture, the quantum Itô equation [14, 17, 18, 31]

$$\begin{aligned} d\hat{a} = dt \sum_{m=1}^M \frac{m}{2} (-\gamma_m \hat{a}^{\dagger m-1} \hat{a}^m + \kappa_m \hat{a}^m \hat{a}^{\dagger m-1}) \\ + \sum_{m=1}^M m \hat{a}^{\dagger m-1} d\hat{W}_m. \end{aligned} \quad (4)$$

The final term showcases the quantum noise explicitly, via the independent operator-valued Wiener increments $d\hat{W}_m$ which satisfy $d\hat{W}_m d\hat{W}_{m'}^\dagger = \delta_{mm'} \gamma_m dt$ and $d\hat{W}_m^\dagger d\hat{W}_{m'} = \delta_{mm'} \kappa_m dt$. The noise operators are necessary to preserve the bosonic commutation relation. Crucially, the noise is additive only for $m = 1$, and multiplicative for all $m > 1$. In the latter case, the noise operator $d\hat{W}_m$ is coupled to the bosonic field $\hat{a}^{\dagger m-1}$. This causes the fluctuations to be self-amplified and grow rapidly, which must be counterbalanced by the damping forces for the steady state to exist. At large excitation numbers, the dominant damping term in Eq. (4) is $\propto (\gamma_M - \kappa_M) \hat{a}^{\dagger M-1} \hat{a}^M$, which vanishes at the critical point $\kappa_M/\gamma_M = 1$. The remaining damping forces can only weakly suppress the fluctuations at large n , which results in the power law tail.

Physical signatures of the power-law tail. — The power-law distribution can be directly observed in experiments by measuring the system in the excitation number basis, such as by photodetection, if the bosonic operator \hat{a} represents an electromagnetic mode. Here, we explore several other physical properties in which the power-law behavior manifests. We restrict the discussion to $M = 2$, which captures most of the essential physics, while analogous results for $M > 2$ are discussed in the SM.

At the critical point $\delta = 0$, the mean occupation number in the steady state is exactly

$$\langle \hat{a}^\dagger \hat{a} \rangle = \frac{1 + \kappa_1/(4\gamma_2)}{\nu - 2}, \quad (5)$$

where $\nu = (\gamma_1 - \kappa_1)/4\gamma_2$ is the power-law exponent.

Equation (5) is valid only for $\nu > 2$ [30], and plotted in Fig. 2(a). The predicted divergence at $\nu = 2$ is consistent with the power-law tail (3). For $\nu < 2$, the mean excitation number $\sim \exp[(2 - \nu)4\gamma_2 t]$ blows up exponentially in time. The second moment can also be computed in the steady state as

$$\langle \hat{a}^{\dagger 2} \hat{a}^2 \rangle = \langle (\hat{a}^\dagger \hat{a})^2 \rangle - \langle \hat{a}^\dagger \hat{a} \rangle^2 = \frac{1 + (8 + \kappa_1/\gamma_2) \langle \hat{a}^\dagger \hat{a} \rangle}{2(\nu - 3)} \quad (6)$$

for $\nu > 3$, and blows up exponentially $\sim \exp[(3 - \nu)8\gamma_2 t]$ for $\nu < 3$. Again, the divergence at $\nu = 3$ is consistent with the power-law tail. All higher moments can be computed recursively [30].

A useful quantity to characterize the bosonic field is the normalized second-order correlation function $g^{(2)}(0) \equiv \langle \hat{a}^{\dagger 2} \hat{a}^2 \rangle / \langle \hat{a}^\dagger \hat{a} \rangle^2$, plotted in Figs. 2(b,c). In the context of an electromagnetic field, $g^{(2)}(0)$ indicates the likelihood of two photons arriving simultaneously at a detector, with $g^{(2)}(0) = 1$ for coherent light described by Poissonian statistics [32]. Incoherent light typically exhibits bunching, i.e., $g^{(2)}(0) > 1$, such as thermal light sources which have $g^{(2)}(0) = 2$. The second-order correlation function can be evaluated from Eqs. (5) and (6) for $\nu > 3$ (setting $\kappa_1 = 0$ for simplicity),

$$g^{(2)}(0) = \frac{(\nu - 2)(\nu + 6)}{2(\nu - 3)}. \quad (7)$$

This has a minimum value of $g^{(2)}(0) = 8$ at $\nu = 6$, which reflects the fact that the steady state is not at thermal equilibrium. $g^{(2)}(0)$ diverges at $\nu = 3$ due to the strong fluctuations in the bosonic field. For $\nu \gg 1$, $g^{(2)}(0) \sim (\nu + 7)/2$ grows linearly with ν [see Fig. 2(c)]. This regime could be accessible in practical implementations where $\{\gamma_2, \kappa_2\} \ll \gamma_1$. Thus, the linear behavior of $g^{(2)}(0)$ can potentially serve as an experimental signature of the power-law tail. We remark that the k -boson correlation function analogous to Eq. (7) scales as $g^{(k)}(0) \equiv \langle \hat{a}^{\dagger k} \hat{a}^k \rangle / \langle \hat{a}^\dagger \hat{a} \rangle^k \sim \nu^{\lfloor k/2 \rfloor}$ for large ν [30].

The behavior of $g^{(2)}(0)$ for $\nu \leq 3$ is less straightforward to analyze. Obviously, the correlation function is infinite in the regime $2 < \nu \leq 3$, since $\langle \hat{a}^\dagger \hat{a} \rangle$ is finite, while $\langle \hat{a}^{\dagger 2} \hat{a}^2 \rangle$ diverges. However, for $\nu \leq 2$, both $\langle \hat{a}^{\dagger 2} \hat{a}^2 \rangle$ and $\langle \hat{a}^\dagger \hat{a} \rangle$ diverge at the critical point. We can gain insights about the physics for $\nu < 2$ using a simple scaling theory [30]: Suppose $\rho_{n,n} \propto n^{-\nu}$ has a sharp cutoff at $n_c = 1/\delta$. A straightforward calculation predicts the scaling behavior $\langle (\hat{a}^\dagger \hat{a})^k \rangle \sim 1/\delta^k$ for $\nu \in (0, 1)$ and $\sim 1/\delta^{k-\nu+1}$ for $\nu \in (1, k+1)$, with $k \in \mathbb{Z}^+$. Consequently, $g^{(2)}(0)$ diverges as $1/\delta^{\nu-1}$ for $\nu \in (1, 2)$. Replacing the sharp cutoff with the exponential cutoff in Eq. (3) only adds a finite correction and does not affect the scaling of the divergences. The predicted divergences from the scaling theory agree with numerical simulations near the critical point, as shown in Fig. 2(b). Note that the observed behavior in Fig. 2(b) cannot be extrapolated to the critical point $\delta = 0$, since $g^{(2)}(0) \sim \exp(8\gamma_2 t)$ blows

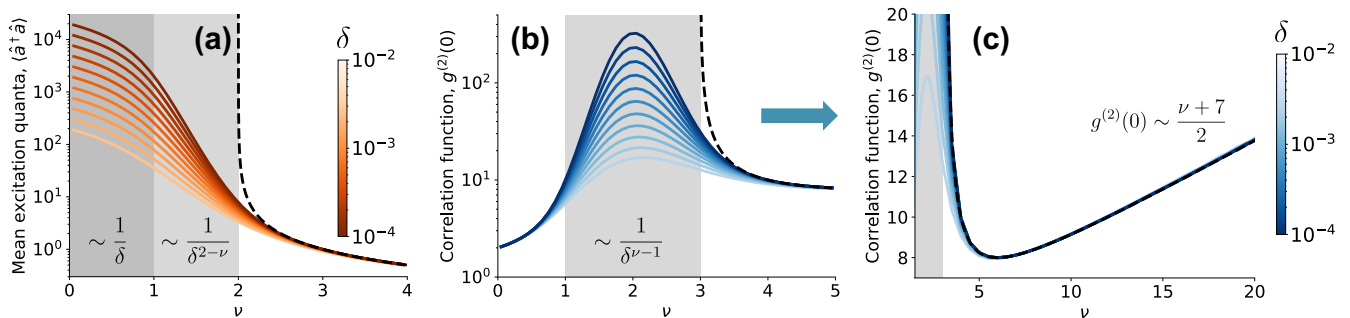


FIG. 2. Physical signatures of the power-law tail in the M -boson model, plotted for $M = 2$ and $\kappa_1 = 0$: (a) Mean number of excitation quanta $\langle \hat{a}^\dagger \hat{a} \rangle$, (b, c) Normalized second-order correlation function $g^{(2)}(0)$. $\delta = 1 - \kappa_2/\gamma_2$ is the deviation from the critical point. The power-law exponent is $\nu = \gamma_1/4\gamma_2$ (3). In all the plots, the solid curves are obtained numerically for $\delta \in [10^{-4}, 10^{-2}]$. The Hilbert space truncation is set at $N_T = 5 \times 10^5$ to ensure numerical convergence. The black dashed lines indicate the corresponding analytical results (5) and (7). Grey shaded regions denote the regime in which the physical quantity is divergent near the critical point, with the divergence derived from the scaling theory indicated. At large ν , $g^{(2)}(0)$ scales linearly with ν .

up exponentially in time for all $\nu < 2$. Mathematically, this corresponds to a singular perturbation. In the regime $\nu \ll \delta$, the steady state is close to thermal equilibrium and thus $g^{(2)}(0) \approx 2$, consistent with the numerical observation.

The power-law behavior can also manifest in the quantum phase space. Introducing the dimensionless quadrature operators $\hat{q} = (\hat{a} + \hat{a}^\dagger)/\sqrt{2}$ and $\hat{p} = -i(\hat{a} - \hat{a}^\dagger)/\sqrt{2}$, with the canonical commutation relation $[\hat{q}, \hat{p}] = i$, we show analytically that the Wigner quasiprobability distribution in the steady state has the asymptotic behavior [30]

$$W(q, p) \sim \frac{1}{(q^2 + p^2)^\nu} \quad (8)$$

with the same power-law exponent ν as the number distribution. This can be observed, for example, by performing tomography on the bosonic mode. If the system represents a quantum particle confined in a one-dimensional harmonic potential, the position and momentum distribution of the particle exhibits the tail behavior $\sim |q|^{1-2\nu}$ and $\sim |p|^{1-2\nu}$ respectively, from Eq. (8).

To summarize, the power-law distribution due to quantum fluctuations gives rise to extreme events which can be orders of magnitude above the typical measured values. As shown above, such effects can be observed through various physical quantities that have a scaling behavior dependent on the power-law exponent ν .

General class of nonlinear dissipative dynamics.— Now, we argue that the power-law behavior is not specific to the M -boson model of Eq. (1), but is instead a generic feature of quantum systems with strong nonlinear dissipation. To this end, we consider a general class

of quantum systems that obey the equation of motion

$$\begin{aligned} \frac{d\langle \hat{q} \rangle}{dt} &= \langle \hat{p} \rangle, \\ \frac{d\langle \hat{p} \rangle}{dt} &= (k_0 \langle \hat{p} \rangle - k_2 \langle : \hat{q}^2 \hat{p} : \rangle) - (k_1 \langle \hat{q} \rangle + k_3 \langle : \hat{q}^3 : \rangle), \end{aligned} \quad (9)$$

reminiscent of the Ehrenfest theorem. Here, \hat{q} and \hat{p} are the quadrature operators defined above, while $\{k_0, k_1, k_2, k_3\}$ are arbitrary non-negative parameters. The notation $\langle : \hat{O} : \rangle$ indicates normal ordering, after expressing the operator \hat{O} in terms of \hat{a} and \hat{a}^\dagger . The choice of operator ordering here is simply for convenience, and does not affect the discussion. Eq. (9) is the quantum analog of the cubic Liénard system. Physically, the parameters k_2 and k_3 represent the nonlinear damping and frequency response (i.e., anharmonicity) of the system, respectively. We seek to ‘quantize’ the Liénard system by constructing a Lindblad master equation that generates the quantum dynamics (9). A general construction for any polynomial dynamical system with a two-dimensional phase space is detailed in Refs. [21, 22]. The resulting master equation is rather complicated, and is included in the SM [30]. The key qualitative difference with the M -boson model (1) is that the dynamical system (9) does not possess continuous rotation symmetry. Therefore, the steady state (if it exists) will contain coherences in the excitation number basis. In the regime of weak nonlinear dissipation $k_2 \ll k_1$, the master equation can be described by a quantum Stuart-Landau model with a generalized squeezing drive [30, 33, 34], which has an exponentially vanishing number distribution. Thus, strong nonlinear dissipation is needed to observe the power-law tail.

We provide numerical evidence for the emergence of power-law tails in the steady state. Unlike the M -boson model (1), the power law in the number distribution $\rho_{n,n}$

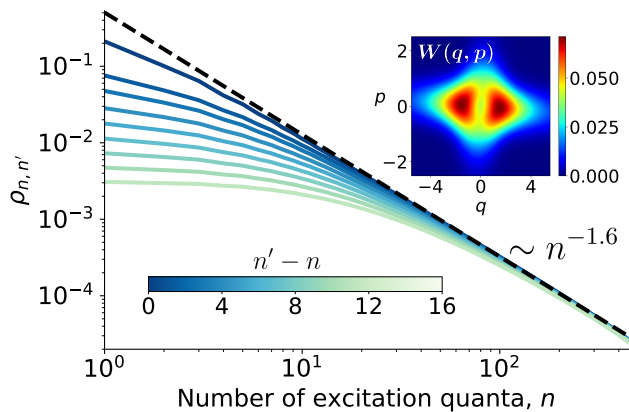


FIG. 3. Magnitudes of density matrix element $|\rho_{n,n'}|$ against the number of excitation quanta n for the quantum Liénard system (9) in the steady state. Curves plotted are for even $n' - n \in [0, 16]$. Matrix elements for odd $n' - n$ are identically zero. The black dashed line shows the power-law scaling $|\rho_{n,n'}| \propto n^{-1.6}$ obtained from numerical fitting the number distribution $\rho_{n,n}$. (Inset) Wigner quasiprobability distribution $W(q, p)$ of the steady state. $W(q, p)$ is mostly supported near the phase space origin, with a heavy tail that decays slowly. Parameters: $(k_0, k_1, k_2, k_3) = (0.169, 0.12, 1, 0.035)$, with a Hilbert space truncation of $N_T = 10^3$ in the numerical simulation for numerical convergence. Similar behavior can be observed for other parameters.

can be observed without fine-tuning of the parameters. We demonstrate this by simulating the master equation with parameters k_0, k_1 and k_3 randomly sampled from $[0, 1]$ (in units of k_2). An explicit example is shown in Fig. 3. Interestingly, the power law does not only emerge in the probabilities $\rho_{n,n}$, like for the M -boson model, but also in the off-diagonal elements (coherences) of the density matrix. In the example shown, we observe the scaling $|\rho_{n,n'}| \sim n^{-1.6}$ for $n' - n$ up to 16. This is in the regime of infinite mean excitation number, akin to $\nu < 2$ in the M -boson model. The physical implication is that extreme

events can be generically observed in quantum systems with strong nonlinear dissipation, due to the amplified quantum fluctuations.

Discussion.— We propose the emergence of power-law distributions and extreme events as a novel universal feature of nonlinear quantum dissipation. This can be understood from the fact that the quantum noise associated with nonlinear dissipation is typically multiplicative in nature. That is, the fluctuations are coupled to the quantum state and become amplified at higher excitation. The competition between dissipation and noise amplification results in the power-law behavior. We introduce the prototypical M -boson model which is analytically proven to produce power-law energy distributions at the critical point. The ubiquity of this phenomenon is further supported via numerical simulations on a general class of nonlinear dynamical systems which are quantum analogs of Liénard systems. We show that power laws can also emerge in the (off-diagonal) coherences of the density matrix, which exhibit the same scaling as the (diagonal) probability distribution.

The power-law behavior can manifest in various observable physical signatures, such as extreme events with divergent mean excitation number, boson superbunching with a divergent $g^{(2)}(0)$ correlation function, and power-law tails in both position and momentum space. This phenomenon opens up potential avenues for exploring extreme regimes of light-matter interactions [35–37], and can be a useful resource for sensing applications like ghost imaging [38, 39]. It would also be interesting as a future theoretical study to connect the results of this work with known mechanisms of the power law [1], such as scale invariance, universality and self-organized criticality.

Acknowledgements.— The author would like to thank Andy Chia, Tobias Haug, Leong-Chuan Kwek, Changsuk Noh, Jingu Pang, John Preskill, Gil Refael and Yu Tong for insightful discussions. The Institute for Quantum Information and Matter is an NSF Physics Frontiers Center.

-
- [1] M. Newman, Power laws, pareto distributions and zipf’s law, *Contemp. Phys.* **46**, 323 (2005).
 - [2] P. A. Marquet, R. A. Quiñones, S. Abades, F. Labra, M. Tognelli, M. Arim, and M. Rivadeneira, Scaling and power-laws in ecological systems, *J. Exp. Biol.* **208**, 1749 (2005).
 - [3] A. Corral and A. González, Power law size distributions in geoscience revisited, *Earth Space Sci.* **6**, 673 (2019).
 - [4] X. Gabaix, Power laws in economics and finance, *Annu. Rev. Econ.* **1**, 255 (2009).
 - [5] C. M. Pinto, A. Mendes Lopes, and J. T. Machado, A review of power laws in real life phenomena, *Commun. Nonlinear Sci. Numer. Simul.* **17**, 3558 (2012).
 - [6] D. Marković and C. Gros, Power laws and self-organized criticality in theory and nature, *Phys. Rep.* **536**, 41 (2014).
 - [7] D. Sornette, L. Knopoff, Y. Y. Kagan, and C. Vanneste, Rank-ordering statistics of extreme events: Application to the distribution of large earthquakes, *J. Geophys. Res. Solid Earth* **101**, 13883 (1996).
 - [8] J. M. Dudley, G. Genty, A. Mussot, A. Chabchoub, and F. Dias, Rogue waves and analogies in optics and oceanography, *Nat. Rev. Phys.* **1**, 675 (2019).
 - [9] E. W. Cliver, C. J. Schrijver, K. Shibata, and I. G. Usoskin, Extreme solar events, *Living Rev. Sol. Phys.* **19**, 2 (2022).
 - [10] X. Gabaix, P. Gopikrishnan, V. Plerou, and H. E. Stanley, A theory of power-law distributions in financial market fluctuations, *Nature* **423**, 267 (2003).
 - [11] J. A. T. Machado and A. M. Lopes, Rare and extreme events: the case of covid-19 pandemic, *Nonlinear Dyn.* **100**, 2953 (2020).

- [12] F. Lillo and R. N. Mantegna, Anomalous spreading of power-law quantum wave packets, *Phys. Rev. Lett.* **84**, 1061 (2000).
- [13] J. Batle, A. Plastino, M. Casas, and A. Plastino, Quantum evolution of power-law mixed states, *Phys. A: Stat. Mech. Appl.* **308**, 233 (2002).
- [14] C. W. Gardiner and P. Zoller, *Quantum Noise*, 2nd ed., edited by H. Haken (Springer, 2000).
- [15] H.-P. Breuer and F. Petruccione, *The Theory of Open Quantum Systems* (Oxford University Press, 2007).
- [16] H. J. Carmichael, *Statistical methods in quantum optics: Vol. 1: Master equations and Fokker-Planck equations; 1st ed., 2nd corr. print*, Texts and monographs in physics (Springer, Berlin, 1999) p. 365 p.
- [17] A. Chia, M. Hajdušek, R. Nair, R. Fazio, L. C. Kwek, and V. Vedral, Phase-preserving linear amplifiers not simulable by the parametric amplifier, *Phys. Rev. Lett.* **125**, 163603 (2020).
- [18] A. Chia, W.-K. D. Mok, C. Noh, and L.-C. Kwek, Quantum pure noise-induced transitions: A truly nonclassical limit cycle sensitive to number parity, *SciPost Phys.* **15**, 121 (2023).
- [19] M. Manceau, K. Y. Spasibko, G. Leuchs, R. Filip, and M. V. Chekhova, Indefinite-mean pareto photon distribution from amplified quantum noise, *Phys. Rev. Lett.* **123**, 123606 (2019).
- [20] K. McNeil and D. Walls, Possibility of observing enhanced photon bunching from two photon emission, *Phys. Lett. A* **51**, 233 (1975).
- [21] W.-K. Mok, *Quantum dynamics of nonlinear dissipative systems*, Bachelor thesis, National University of Singapore (2022).
- [22] A. Chia, W.-K. Mok, L.-C. Kwek, and C. Noh, Quantisation of nonlinear non-hamiltonian systems, (in preparation).
- [23] S. H. Strogatz, *Nonlinear Dynamics and Chaos: With Applications to Physics, Biology, Chemistry and Engineering* (Westview Press, 2000).
- [24] S. Walter, A. Nunnenkamp, and C. Bruder, Quantum synchronization of a driven self-sustained oscillator, *Phys. Rev. Lett.* **112**, 094102 (2014).
- [25] S. Walter, A. Nunnenkamp, and C. Bruder, Quantum synchronization of two van der pol oscillators, *Ann. Phys. (Berlin)* **527**, 131 (2015).
- [26] N. Lörch, E. Amitai, A. Nunnenkamp, and C. Bruder, Genuine quantum signatures in synchronization of anharmonic self-oscillators, *Phys. Rev. Lett.* **117**, 073601 (2016).
- [27] W.-K. Mok, L.-C. Kwek, and H. Heimonen, Synchronization boost with single-photon dissipation in the deep quantum regime, *Phys. Rev. Res.* **2**, 033422 (2020).
- [28] Z. Leghtas, S. Touzard, I. M. Pop, A. Kou, B. Vlastakis, A. Petrenko, K. M. Sliwa, A. Narla, S. Shankar, M. J. Hatridge, M. Reagor, L. Frunzio, R. J. Schoelkopf, M. Mirrahimi, and M. H. Devoret, Confining the state of light to a quantum manifold by engineered two-photon loss, *Science* **347**, 853 (2015).
- [29] R. Lescanne, M. Villiers, T. Peronmin, A. Sarlette, M. Delbecq, B. Huard, T. Kontos, M. Mirrahimi, and Z. Leghtas, Exponential suppression of bit-flips in a qubit encoded in an oscillator, *Nat. Phys.* **16**, 509 (2020).
- [30] See Supplementary Materials for additional calculation details, which includes Refs. [40, 41].
- [31] R. L. Hudson and K. R. Parthasarathy, Quantum Ito's formula and stochastic evolutions, *Commun. Math. Phys.* **93**, 301 (1984).
- [32] L. Mandel and E. Wolf, *Optical Coherence and Quantum Optics* (Cambridge University Press, 1995).
- [33] S. Sonar, M. Hajdušek, M. Mukherjee, R. Fazio, V. Vedral, S. Vinjanampathy, and L.-C. Kwek, Squeezing enhances quantum synchronization, *Phys. Rev. Lett.* **120**, 163601 (2018).
- [34] Y. Shen, W.-K. Mok, C. Noh, A. Q. Liu, L.-C. Kwek, W. Fan, and A. Chia, Quantum synchronization effects induced by strong nonlinearities, *Phys. Rev. A* **107**, 053713 (2023).
- [35] J. Heimerl, A. Mikhaylov, S. Meier, H. Höllerer, I. Kaminer, M. Chekhova, and P. Hommelhoff, Multiphoton electron emission with non-classical light, *Nature Physics* **20**, 945 (2024).
- [36] P. Stammer, J. Rivera-Dean, A. Maxwell, T. Lamprou, A. Ordóñez, M. F. Ciappina, P. Tzallas, and M. Lewenstein, Quantum electrodynamics of intense laser-matter interactions: A tool for quantum state engineering, *PRX Quantum* **4**, 010201 (2023).
- [37] A. Gorlach, M. E. Tzur, M. Birk, M. Krüger, N. Rivera, O. Cohen, and I. Kaminer, High-harmonic generation driven by quantum light, *Nat. Phys.* **19**, 1689 (2023).
- [38] A. Gatti, E. Brambilla, M. Bache, and L. A. Lugiato, Ghost imaging with thermal light: Comparing entanglement and classical correlation, *Phys. Rev. Lett.* **93**, 093602 (2004).
- [39] K. W. C. Chan, M. N. O'Sullivan, and R. W. Boyd, High-order thermal ghost imaging, *Opt. Lett.* **34**, 3343 (2009).
- [40] L. Ben Arosh, M. C. Cross, and R. Lifshitz, Quantum limit cycles and the rayleigh and van der pol oscillators, *Phys. Rev. Res.* **3**, 013130 (2021).
- [41] P. D. Drummond and M. Hillery, *The Quantum Theory of Nonlinear Optics* (Cambridge University Press, 2014).

Supplemental Material

We provide additional technical details supporting the claims in the main text.

CONTENTS

I. Steady state number distribution for the M -boson model	7
II. Analytical results for $M = 2$ at the critical point	8
A. Moments of the number distribution	8
B. Higher-order bosonic correlation function	10
C. Wigner quasiprobability distribution	10
III. Scaling behavior of the number statistics	12
IV. Quantum Liénard system	13
A. ‘Quantization’ of dissipative dynamical systems	14
B. Example: Cubic Liénard system	14

I. STEADY STATE NUMBER DISTRIBUTION FOR THE M -BOSON MODEL

Consider the M -boson model, with the Lindblad master equation

$$\dot{\rho} = -i[\omega_0 \hat{a}^\dagger \hat{a}, \rho] + \sum_{m=1}^M (\gamma_m \mathcal{D}[\hat{a}^m] \rho + \kappa_m \mathcal{D}[\hat{a}^{\dagger m}] \rho). \quad (1)$$

This describes a quantum harmonic oscillator subject to incoherent processes such as damping (governed by the γ_m terms) and pumping (governed by the κ_m terms). On top of the harmonic oscillator Hamiltonian $H_0 = \hbar\omega_0 \hat{a}^\dagger \hat{a}$, one can also consider a generalized model by adding any Hamiltonian which is diagonal in the number (Fock) basis $\{|n\rangle\}$. This includes, for example, a Kerr nonlinearity $H_{\text{Kerr}} = K \hat{a}^{\dagger 2} \hat{a}^2$ which controls the anharmonicity of the oscillator. Such terms do not contribute to the dynamics of the populations (diagonal elements of ρ in the number basis),

$$\begin{aligned} \dot{\rho}_{n,n} = & \sum_{m=1}^M \gamma_m \left[\rho_{n+m,n+m} \prod_{j=1}^m (n+j) - \rho_{n,n} \prod_{j=0}^{m-1} (n-j) \right] \\ & + \sum_{m=1}^M \kappa_m \left[\rho_{n-m,n-m} \prod_{j=0}^{m-1} (n-j) - \rho_{n,n} \prod_{j=1}^m (n+j) \right], \end{aligned} \quad (2)$$

as given in the main text. For $M = 2$, the exact solution to the steady state populations can be found in Ref. [40]. However, the solution is a complicated expression in terms of hypergeometric functions, and is cumbersome to work with. Here, we are interested in the asymptotic behavior of $\rho_{n,n}$ for large n . To this end, we propose the truncated power-law ansatz

$$\rho_{n,n} \propto \frac{e^{-n/\xi}}{n^\nu}, \quad (3)$$

for large n , where ξ and ν are to be determined. This gives the relation

$$\rho_{n+m,n+m} = \rho_{n,n} e^{-m/\xi} \left(1 + \frac{m}{n}\right)^{-\nu} = \rho_{n,n} e^{-m/\xi} \left(1 - \frac{\nu m}{n} + \frac{\nu(\nu-1)m^2}{2n^2} + \dots\right) \quad (4)$$

between the populations. Substituting Eq. (4) into the steady state condition $\dot{\rho}_{n,n} = 0$, we obtain

$$\begin{aligned} 0 = & \sum_{m=1}^M \gamma_m n^m \left[e^{-m/\xi} \left(1 + \frac{m(m+1-2\nu)}{2n} + \dots\right) - \left(1 - \frac{m(m-1)}{2n} + \dots\right) \right] \\ & + \sum_{m=1}^M \kappa_m n^m \left[e^{m/\xi} \left(1 - \frac{m(m-1-2\nu)}{2n} + \dots\right) - \left(1 + \frac{m(m+1)}{2n} + \dots\right) \right]. \end{aligned} \quad (5)$$

To leading order $\mathcal{O}(n^M)$, we have

$$\gamma_M \left(e^{-M/\xi} - 1 \right) + \kappa_M \left(e^{M/\xi} - 1 \right) = 0 \quad (6)$$

which can be readily solved to yield

$$\xi = \frac{M}{\ln(\gamma_M/\kappa_M)}. \quad (7)$$

Let us write $\delta = 1 - \kappa_M/\gamma_M$, where $\delta \geq 0$ is required for the steady state to exist. Near the critical point $\delta = 0$, we can write

$$\xi = \frac{M}{-\ln(1-\delta)} \approx \frac{M}{\delta}. \quad (8)$$

The parameter ξ controls the onset of the exponential cutoff, which occurs roughly at $n \sim \xi \approx M/\delta$. As $\delta \rightarrow 0^+$, the exponential cutoff becomes irrelevant, and the number distribution $\rho_{n,n} \sim n^{-\nu}$ exhibits a power-law tail. To obtain the power-law exponent ν , we consider Eq. (5) to the subleading order $\mathcal{O}(n^{M-1})$, which gives

$$\begin{aligned} & \frac{\gamma_M}{2} \left(e^{-M/\xi} M(M+1-2\nu) + M(M-1) \right) + \gamma_{M-1} \left(e^{-(M-1)/\xi} - 1 \right) \\ & - \frac{\kappa_M}{2} \left(e^{M/\xi} M(M-1-2\nu) + M(M+1) \right) + \kappa_{M-1} \left(e^{(M-1)/\xi} - 1 \right) = 0. \end{aligned} \quad (9)$$

For small δ , we can solve for ν approximately to get the power-law exponent

$$\nu \approx \frac{M-1}{M^2} \frac{\gamma_{M-1} - \kappa_{M-1}}{\gamma_M - \kappa_M} \delta = \frac{M-1}{M^2} \frac{\gamma_{M-1} - \kappa_{M-1}}{\gamma_M} \delta \quad (10)$$

as stated in the main text. To summarize, near the critical point, the number distribution has a truncated power-law of the form

$$\boxed{\rho_{n,n} \propto \frac{e^{-n\delta/M}}{n^\nu}}, \quad (11)$$

where ν is given in Eq. (10). At $\delta = 0$, the exponential cutoff vanishes, and the distribution exhibits a power-law tail for arbitrarily large n .

II. ANALYTICAL RESULTS FOR $M = 2$ AT THE CRITICAL POINT

Here, we present additional analytical results for the M -boson model.

A. Moments of the number distribution

From the master equation for the M -boson model, the equation of motion for a general observable \hat{O} is given by

$$\frac{d\langle \hat{O} \rangle}{dt} = \text{Tr} \left(\hat{O} \dot{\rho} \right) = i\omega_0 \langle [\hat{a}^\dagger \hat{a}, \hat{O}] \rangle + \sum_{m=1}^M \frac{\gamma_m}{2} \left(\langle \hat{a}^{\dagger m} [\hat{O}, \hat{a}^m] \rangle + \langle [\hat{a}^{\dagger m}, \hat{O}] \hat{a}^m \rangle \right) + \frac{\kappa_m}{2} \left(\langle \hat{a}^m [\hat{O}, \hat{a}^{\dagger m}] \rangle + \langle [\hat{a}^m, \hat{O}] \hat{a}^{\dagger m} \rangle \right). \quad (12)$$

Let us consider the case of $M = 2$, which is the minimal model for observing the power-law behavior. We denote the excitation number operator as $\hat{n} = \hat{a}^\dagger \hat{a}$. Setting $\hat{O} = \hat{a}^\dagger \hat{a}$ in Eq. (12), and using the commutation relation $[\hat{a}, \hat{a}^\dagger] = 1$, yields the equation of motion

$$\frac{d\langle \hat{n} \rangle}{dt} = \kappa_1 + 4\kappa_2 + (-\gamma_1 + \kappa_2 + 2\gamma_2 + 6\kappa_2) \langle \hat{n} \rangle - 2(\gamma_2 - \kappa_2) \langle \hat{n}^2 \rangle. \quad (13)$$

At the critical point, i.e., $\gamma_2 = \kappa_2$, the mean excitation number $\langle \hat{n}(t) \rangle$ can be solved exactly to give

$$\langle \hat{n}(t) \rangle = \langle \hat{n}(0) \rangle e^{-(\gamma_1 - \kappa_1 - 8\gamma_2)t} + \frac{\kappa_1 + 4\gamma_2}{\gamma_1 - \kappa_1 - 8\gamma_2} \left[1 - e^{-(\gamma_1 - \kappa_1 - 8\gamma_2)t} \right]. \quad (14)$$

In terms of the power-law exponent

$$\nu = \frac{\gamma_1 - \kappa_1}{4\gamma_2} \quad (15)$$

from Eq. (10), the mean excitation number can be written as

$$\langle \hat{n}(t) \rangle = \langle \hat{n}(0) \rangle e^{-4(\nu-2)\gamma_2 t} + \frac{1 + \kappa_1/4\gamma_2}{\nu - 2} \left[1 - e^{-4(\nu-2)\gamma_2 t} \right]. \quad (16)$$

Clearly, if $\nu < 2$, $\langle \hat{n}(t) \rangle \sim \exp[4(2 - \nu)\gamma_2 t]$ diverges exponentially in time. Next, we set $\hat{O} = \hat{n}^2$. At the critical point, we have the equation of motion

$$\frac{d\langle \hat{n}^2 \rangle}{dt} = \kappa_1 + 8\gamma_2 + (\gamma_1 + 3\kappa_1 + 16\gamma_2) \langle \hat{n} \rangle + 2(-\gamma_1 + \kappa_1 + 12\gamma_2) \langle \hat{n}^2 \rangle. \quad (17)$$

The solution for $\langle \hat{n}^2(t) \rangle$ is given by

$$\langle \hat{n}^2(t) \rangle = \langle \hat{n}^2(0) \rangle e^{-8(\nu-3)\gamma_2 t} + \frac{1 + \kappa_1/8\gamma_2}{\nu - 3} \left[1 - e^{-8(\nu-3)\gamma_2 t} \right] + (\gamma_1 + 3\kappa_1 + 16\gamma_2) \int_0^t dt' \langle \hat{n}(t') \rangle e^{8(\nu-3)\gamma_2(t'-t)}. \quad (18)$$

The integral in the final term can be evaluated explicitly by substituting the expression for $\langle \hat{n}(t) \rangle$ from Eq. (16), although the resulting expression is rather complicated. By inspection, the expression has the form

$$\langle \hat{n}^2(t) \rangle = \frac{3}{2} \frac{(1 + \kappa_1/4\gamma_2)(1 + \kappa_1/6\gamma_2)}{(\nu - 2)(\nu - 3)} + C_1 e^{-4(\nu-2)\gamma_2 t} + C_2 e^{-8(\nu-3)\gamma_2 t} \quad (19)$$

for some coefficients C_1 and C_2 . Thus, for $\nu < 3$, $\langle \hat{n}^2(t) \rangle \sim \exp[8(3 - \nu)\gamma_2 t]$ diverges exponentially in time. The divergences in $\langle \hat{n}(t) \rangle$ and $\langle \hat{n}^2(t) \rangle$ are consistent with the power-law behavior.

We now derive a recurrence relation for the steady state expectation values $\langle \hat{a}^{\dagger k} \hat{a}^k \rangle$, assuming $\nu > k + 1$ such that the steady state values exist. These can be converted to steady state values for the moments $\langle \hat{n}^k \rangle$ of the number distribution.

Setting $\hat{O} = \hat{a}^{\dagger k} \hat{a}^k$ in Eq. (12) gives the equation of motion

$$\begin{aligned} \frac{d\langle \hat{a}^{\dagger k} \hat{a}^k \rangle}{dt} &= \frac{\gamma_1}{2} (\langle \hat{a}^{\dagger} [\hat{a}^{\dagger k} \hat{a}^k, a] \rangle + \langle [\hat{a}^{\dagger}, \hat{a}^{\dagger k} \hat{a}^k] \hat{a} \rangle) \\ &+ \frac{\kappa_1}{2} (\langle \hat{a} [\hat{a}^{\dagger k} \hat{a}^k, \hat{a}^{\dagger}] \rangle + \langle [\hat{a}, \hat{a}^{\dagger k} \hat{a}^k] \hat{a}^{\dagger} \rangle) \\ &+ \frac{\gamma_2}{2} (\langle \hat{a}^{\dagger 2} [\hat{a}^{\dagger k} \hat{a}^k, \hat{a}^2] \rangle + \langle [\hat{a}^{\dagger 2}, \hat{a}^{\dagger k} \hat{a}^k] \hat{a}^2 \rangle) \\ &+ \frac{\kappa_2}{2} (\langle \hat{a}^2 [\hat{a}^{\dagger k} \hat{a}^k, \hat{a}^{\dagger 2}] \rangle + \langle [\hat{a}^2, \hat{a}^{\dagger k} \hat{a}^k] \hat{a}^{\dagger 2} \rangle). \end{aligned} \quad (20)$$

Using the identities $[\hat{a}, \hat{a}^{\dagger k}] = k\hat{a}^{\dagger k-1}$ and $[\hat{a}^2, \hat{a}^{\dagger k}] = 2k\hat{a}^{\dagger k-1}\hat{a} + k(k-1)\hat{a}^{\dagger k-2}$, which can be derived from the bosonic commutation relation, we obtain

$$\begin{aligned} \frac{d\langle \hat{a}^{\dagger k} \hat{a}^k \rangle}{dt} &= k^2(k-1)^2\kappa_2 \langle \hat{a}^{\dagger k-2} \hat{a}^{k-2} \rangle + k^2(\kappa_1 + 4k\kappa_2) \langle \hat{a}^{\dagger k-1} \hat{a}^{k-1} \rangle \\ &- k[\gamma_1 - \kappa_1 - (k-1)(\gamma_2 - \kappa_2) - 4(k+1)\kappa_2] \langle \hat{a}^{\dagger k} \hat{a}^k \rangle - 2k(\gamma_2 - \kappa_2) \langle \hat{a}^{\dagger k+1} \hat{a}^{k+1} \rangle. \end{aligned} \quad (21)$$

In the steady state, this gives a recurrence relation for $\langle \hat{a}^{\dagger k} \hat{a}^k \rangle$. At the critical point, $\kappa_2 = \gamma_2$, we have

$$\langle \hat{a}^{\dagger k} \hat{a}^k \rangle = \frac{k}{\nu - (k+1)} \left[\left(k + \frac{\kappa_1}{4\gamma_2} \right) \langle \hat{a}^{\dagger k-1} \hat{a}^{k-1} \rangle + \left(\frac{k-1}{2} \right)^2 \langle \hat{a}^{\dagger k-2} \hat{a}^{k-2} \rangle \right] \quad (22)$$

valid for $k \in \mathbb{Z}^+$ and $\nu > k + 1$. As an application of this formula, we now derive asymptotic expressions for bosonic correlation functions at large ν .

B. Higher-order bosonic correlation function

The k -th order bosonic correlation function (at zero delay) is defined as

$$g^{(k)}(0) \equiv \frac{\langle \hat{a}^{\dagger k} \hat{a}^k \rangle}{\langle \hat{a}^{\dagger} \hat{a} \rangle^k} \quad (23)$$

evaluated at the steady state. If we regard the system as a photon source, $g^{(k)}(0)$ can be interpreted as a measure of the likelihood for k photons to be emitted simultaneously, i.e., k -photon bunching.

Taking the limit $\nu \rightarrow \infty$, and using the recurrence relation (22), we have the asymptotic expressions

$$\begin{aligned} \langle \hat{a}^{\dagger} \hat{a} \rangle &\sim \frac{1}{\nu}, & \langle \hat{a}^{\dagger 2} \hat{a}^2 \rangle &\sim \frac{1}{2\nu} \\ \langle \hat{a}^{\dagger 3} \hat{a}^3 \rangle &\sim \frac{15}{2\nu^2}, & \langle \hat{a}^{\dagger 4} \hat{a}^4 \rangle &\sim \frac{9}{2\nu^2} \\ \langle \hat{a}^{\dagger 5} \hat{a}^5 \rangle &\sim \frac{525}{2\nu^3}, & \langle \hat{a}^{\dagger 6} \hat{a}^6 \rangle &\sim \frac{675}{4\nu^3} \\ \langle \hat{a}^{\dagger 7} \hat{a}^7 \rangle &\sim \frac{99225}{4\nu^4}, & \langle \hat{a}^{\dagger 8} \hat{a}^8 \rangle &\sim \frac{33075}{2\nu^4}. \end{aligned} \quad (24)$$

We can derive general asymptotic expressions for $\langle \hat{a}^{\dagger k} \hat{a}^k \rangle$. Observe that for even k , the dominant contribution on the right hand side of Eq. (22) comes from $\langle \hat{a}^{\dagger k-2} \hat{a}^{k-2} \rangle$. Therefore, setting $k = 2l$ we have the asymptotic recurrence relation for the even moments:

$$\langle \hat{a}^{\dagger 2l} \hat{a}^{2l} \rangle \sim \frac{2l}{\nu} \left(\frac{2l-1}{2} \right)^2 \langle \hat{a}^{\dagger 2l-2} \hat{a}^{2l-2} \rangle, \quad (25)$$

which can be solved to yield

$$\boxed{\langle \hat{a}^{\dagger 2l} \hat{a}^{2l} \rangle \sim \frac{l!(2l-1)!!^2}{2^l \nu^l}}. \quad (26)$$

For odd k , the contributions from $\langle \hat{a}^{\dagger k-1} \hat{a}^{k-1} \rangle$ and $\langle \hat{a}^{\dagger k-2} \hat{a}^{k-2} \rangle$ on the right hand side of Eq. (22) are comparable. Setting $k = 2l + 1$, we have the asymptotic recurrence relation

$$\langle \hat{a}^{\dagger 2l+1} \hat{a}^{2l+1} \rangle \sim \frac{2l+1}{\nu} \left[l^2 \langle \hat{a}^{\dagger 2l-1} \hat{a}^{2l-1} \rangle + \frac{l!(2l-1)!!^2 (2l+1)}{2^l \nu^l} \right] \quad (27)$$

where we used Eq. (26). This can be solved by making the ansatz $\langle \hat{a}^{\dagger 2l+1} \hat{a}^{2l+1} \rangle \sim f(l) \nu^{-(l+1)}$ for some function $f(l)$ to be determined, and the result is

$$\boxed{\langle \hat{a}^{\dagger 2l+1} \hat{a}^{2l+1} \rangle \sim \frac{(l+1)!(2l+1)!!^2 (2l+3)}{3(l+1)2^l \nu^{l+1}}}. \quad (28)$$

Substituting the asymptotic expressions into the definition of $g^{(k)}(0)$ (23) gives

$$g^{(k)}(0) \propto \nu^{\lfloor k/2 \rfloor} \quad (29)$$

for large ν . This can be used potentially as an experimental signature of the power-law behavior.

C. Wigner quasiprobability distribution

As stated in the main text, we define the quadrature operators

$$\hat{q} = \frac{1}{\sqrt{2}} (\hat{a} + \hat{a}^{\dagger}), \quad \hat{p} = -\frac{i}{\sqrt{2}} (\hat{a} - \hat{a}^{\dagger}) \quad (30)$$

satisfying the canonical commutation relation $[\hat{q}, \hat{p}] = i$. If the system physically describes a quantum particle trapped in a one-dimensional potential, \hat{q} and \hat{p} are the dimensionless position and momentum operators.

The quantum state ρ can be represented in phase space by the Wigner quasiprobability distribution $W(q, p)$ [14–16]. For the M -boson model, the steady state Wigner distribution is rotationally symmetric. Thus, it is more convenient to work with $W(\alpha, \alpha^*)$, where $\alpha = (q + ip)/\sqrt{2}$ is the complex amplitude. The Lindblad master equation (1) can be converted to an equation of motion for the Wigner distribution. To perform this conversion, it is helpful to recall the operator mapping dictionary [41]

$$\begin{aligned}\hat{a}\rho &\longrightarrow \left(\alpha + \frac{1}{2}\partial_{\alpha^*}\right)W(\alpha, \alpha^*) \equiv D_1W(\alpha, \alpha^*), & \rho\hat{a}^\dagger &\longrightarrow D_1^*W(\alpha, \alpha^*) \\ \rho\hat{a} &\longrightarrow \left(\alpha - \frac{1}{2}\partial_{\alpha^*}\right)W(\alpha, \alpha^*) \equiv D_2W(\alpha, \alpha^*), & \hat{a}^\dagger\rho &\longrightarrow D_2^*W(\alpha, \alpha^*)\end{aligned}\quad (31)$$

which maps the bosonic operators (which act in Hilbert space) to differential operators (which act in phase space), denoted by D_1 and D_2 . It can be checked that the differential operators satisfy the commutation relations

$$[D_1, D_1^*] = [D_2, D_2^*] = [D_1, D_2] = 0 \quad (32)$$

and

$$[D_1, D_2^*] = 1. \quad (33)$$

We can further exploit the rotational symmetry of the model by writing

$$W(\alpha, \alpha^*) = W(r), \quad r = |\alpha|, \quad (34)$$

since the steady state Wigner distribution only depends on the radial coordinate $r = |\alpha|$. The Wigner distribution is normalized as follows:

$$1 = \int d\alpha d\alpha^* W(\alpha, \alpha^*) = 2\pi \int_0^\infty dr r W(r). \quad (35)$$

It is convenient to work with the coordinate $R \equiv r^2$, such that $W(R) \equiv W(r = \sqrt{R})$. We have the useful identities

$$\alpha\partial_\alpha = \alpha^*\partial_{\alpha^*} = R\partial_R, \quad \partial_\alpha\partial_{\alpha^*} = \partial_R R\partial_R. \quad (36)$$

Using the operator mapping dictionary, one can show that the steady state Wigner distribution $W(R)$ satisfies the differential equation

$$0 = (\gamma_1 - \kappa_1)(1 + R\partial_R)W + \frac{\gamma_1 + \kappa_1}{2}\partial_R R\partial_R W + (\gamma_2 - \kappa_2)\left(4R + 2R^2\partial_R + \frac{1}{2}R\partial_R^2 R\partial_R\right)W + 2(\gamma_2 + \kappa_2)(R\partial_R + R\partial_R R\partial_R)W. \quad (37)$$

At the critical point $\kappa_2 = \gamma_2$, this simplifies to

$$0 = (\gamma_1 - \kappa_1)(1 + R\partial_R)W + \frac{\gamma_1 + \kappa_1}{2}\partial_R R\partial_R W + 4\gamma_2(R\partial_R + R\partial_R R\partial_R)W. \quad (38)$$

Substituting the ansatz

$$W(R) \propto \frac{1}{R^\nu}, \quad (39)$$

where ν is to be determined, we have

$$0 = (\gamma_1 - \kappa_1)\frac{1 - \nu}{R^\nu} + \frac{\gamma_1 + \kappa_1}{2}\frac{\nu^2}{R^{\nu+1}} + \frac{4\gamma_2\nu(\nu - 1)}{R^\nu}. \quad (40)$$

For large R , we obtain

$$\nu \approx \frac{\gamma_1 - \kappa_1}{4\gamma_2} \quad (41)$$

which is exactly the power-law exponent (10) for the number distribution. The other solution $\nu = 1$ is unphysical, since it leads to non-normalizable Wigner distributions.

In terms of the phase space coordinates q and p , we have the tail behavior

$$W(q, p) \propto \frac{1}{(q^2 + p^2)^\nu}, \quad (42)$$

as stated in the main text. The probability distribution for the quadrature can be obtained by taking the marginal of $W(q, p)$. For example,

$$P(q) = \int_{-\infty}^{\infty} dp W(q, p) \propto \frac{1}{q^{2\nu-1}}, \quad (43)$$

and similarly for $P(p)$.

III. SCALING BEHAVIOR OF THE NUMBER STATISTICS

Here, we derive analytical predictions for the divergences of the various statistics presented in the main text, such as the mean number of excitation quanta and the second-order correlation function, as we approach the critical point $\delta \rightarrow 0^+$. While the numerical results shown in the main text are for special case of $M = 2$, the analytical treatment here holds for the general M -boson model.

To obtain the scaling behavior in terms of δ , we can use the asymptotic behavior of $\rho_{n,n}$ derived in Eq. (11). However, the analysis can be made much simpler by considering the continuous probability distribution

$$p(n) = \begin{cases} An^{-\nu}, & n \in [1, \frac{1}{\delta}] \\ 0, & \text{else} \end{cases} \quad (44)$$

where A is a normalization factor. We regard $p(n)$ as a proxy for the discrete distribution $\rho_{n,n}$. The exponential cutoff for $\rho_{n,n}$ at $n \sim 1/\delta$ is replaced by a sharp cutoff for $p(n)$ at $n = 1/\delta$. The main idea is that the divergences in the number statistics can only arise from the power-law behavior of $\rho_{n,n}$. Thus, the scaling predictions from analyzing $p(n)$ will be qualitatively correct. Similarly, approximating the discrete distribution by a continuous distribution does not affect the qualitative nature of the divergences stemming from the power-law.

The normalization factor A can be evaluated as

$$A = \begin{cases} \frac{\nu - 1}{1 - \delta^{\nu-1}}, & \nu > 0 \text{ and } \nu \neq 1 \\ \frac{1}{\log(1/\delta)}, & \nu = 1 \end{cases} \quad (45)$$

which vanishes as $\delta^{1-\nu}$ for $0 < \nu < 1$ and is finite for $\nu > 1$. For $k \in \mathbb{Z}^+$, the k -th moment of the distribution $p(n)$ is given by

$$\langle n^k \rangle = A \int_1^{1/\delta} dn n^{k-\nu} = \frac{A}{k - \nu + 1} \left(\frac{1}{\delta^{k-\nu+1}} - 1 \right) \quad (46)$$

if $\nu \neq k + 1$, and $\langle n^k \rangle = A \log(1/\delta)$ if $\nu = k + 1$. This yields the scaling behavior (as $\delta \rightarrow 0^+$)

$$\langle n^k \rangle \sim \begin{cases} \frac{1}{\delta^k}, & 0 < \nu < 1 \\ \frac{1}{\delta^k \log(1/\delta)}, & \nu = 1 \\ \frac{1}{\delta^{k-\nu+1}}, & 1 < \nu < k + 1 \\ \log(1/\delta), & \nu = k + 1 \\ \text{finite}, & \nu > k + 1 \end{cases} \quad (47)$$

We can use this to derive the scaling behavior of the normalized second-order correlation function

$$g^{(2)}(0) = \frac{\langle n^2 \rangle - \langle n \rangle^2}{\langle n \rangle^2} \sim \begin{cases} \text{finite}, & 0 < \nu < 1 \\ \log(1/\delta), & \nu = 1 \\ \frac{1}{\delta^{\nu-1}}, & 1 < \nu < 2 \\ \frac{1}{\delta^{3-\nu} \log^2(1/\delta)}, & \nu = 2 \\ \log(1/\delta), & \nu = 3 \\ \text{finite}, & \nu > 3 \end{cases} \quad (48)$$

which is divergent in the regime $1 \leq \nu \leq 3$. This is consistent with the numerical results shown in the main text.

IV. QUANTUM LIÉNARD SYSTEM

The quantum Liénard system, proposed in Refs. [21, 22], serves as a quantum mechanical analog to the (classical) Liénard system, which is well-studied in the context of nonlinear dynamics. The general Liénard system is given by the dynamical equations

$$\begin{aligned} \dot{q} &= p, \\ \dot{p} &= -f(q)p - g(q) \end{aligned} \quad (49)$$

defined on a two-dimensional phase space with coordinates (q, p) . Physically, q and p can be thought of as the position and momentum of a particle moving on a line. $f(q)$ and $g(q)$ are real and continuously differentiable functions. Liénard's theorem [23] guarantees that the system has a unique and stable limit cycle surrounding the phase space origin if the following conditions are satisfied:

1. g is an odd function, i.e. $g(-q) = -g(q)$.
2. f is an even function, i.e. $f(-q) = f(q)$.
3. $g(q) > 0$ for $q > 0$.
4. $F(q) \equiv \int_0^q f(u)du$ has exactly one positive root at some $q = a$, negative for $0 < q < a$, positive and nondecreasing for $q > a$.

Notable examples of dynamical systems that satisfy Liénard's theorem include paradigmatic models such as the van der Pol, Rayleigh, and Duffing oscillators.

Inspired by Eq. (49), we consider the quantum equation of motion

$$\begin{aligned} \frac{d\langle \hat{q} \rangle}{dt} &= \langle \hat{p} \rangle \\ \frac{d\langle \hat{p} \rangle}{dt} &= -\langle : f(\hat{q}) \hat{p} : \rangle - \langle : g(\hat{q}) : \rangle \end{aligned} \quad (50)$$

where \hat{q} and \hat{p} are the quadrature operators from Eq. (30). The notation $\langle : \hat{O} : \rangle$ indicates normal ordering, after expressing the operator \hat{O} in terms of \hat{a} and \hat{a}^\dagger . Here, we restrict to the case where f and g are at most cubic polynomials. In this restricted setting, the most general system that satisfies Liénard's theorem, and thus guaranteed to be classically stable, has

$$f(q) = -k_0 + k_2 q^2, \quad g(q) = k_1 q + k_3 q^3, \quad (51)$$

where $\{k_0, k_1, k_2, k_3\}$ are non-negative parameters. This corresponds to the model stated in the main text.

A. ‘Quantization’ of dissipative dynamical systems

Eq. (50) cannot be simulated directly, since the system of equations is not closed in general. Instead, we seek a generator of infinitesimal time translation in the form of a Lindblad master equation. A general construction of the master equation (referred to as ‘quantization’) for an arbitrary polynomial f and g can be found in Refs. [21, 22]. For completeness, we briefly summarize the steps involved in the ‘quantization’ procedure:

1. Start with the classical equation of motion of interest, of the form

$$\dot{q} = f_1(q, p), \quad \dot{p} = f_2(q, p), \quad (52)$$

where f_1 and f_2 are arbitrary polynomial functions.

2. Introduce the classical complex variable $\alpha = (q + ip)/\sqrt{2}$, which has the equation of motion

$$\dot{\alpha} = \frac{1}{\sqrt{2}} [f_1(\alpha, \alpha^*) + i f_2(\alpha, \alpha^*)], \quad (53)$$

where $f_1(\alpha, \alpha^*) \equiv f_1(q = (\alpha + \alpha^*)/\sqrt{2}, p = -i(\alpha - \alpha^*)/\sqrt{2})$ (with a slight abuse of notation), and similarly defined for $f_2(\alpha, \alpha^*)$.

3. Since α is a classical variable (sometimes called a c -number), we can change the order of α and α^* freely in $f_1(\alpha, \alpha^*)$ and $f_2(\alpha, \alpha^*)$. For convenience, reorder the terms such that all the α^* appears on the left of α .
4. Making the substitution $\alpha \rightarrow \hat{a}$ and $\alpha^* \rightarrow \hat{a}^\dagger$, we can write down the quantum equation of motion

$$\frac{d\langle \hat{a} \rangle}{dt} = \frac{1}{\sqrt{2}} [\langle : f_1(\hat{a}, \hat{a}^\dagger) : \rangle + i \langle : f_2(\hat{a}, \hat{a}^\dagger) : \rangle]. \quad (54)$$

The normal ordering of operators comes from Step 3. The choice of ordering here is simply for convenience. In principle, the master equation can be constructed for any arbitrary operator ordering.

5. Construct a Lindblad master equation

$$\dot{\rho} = -i[\hat{H}, \rho] + \sum_j \Gamma_j \mathcal{D}[\hat{c}_j] \rho \quad (55)$$

for a suitable (and in general non-unique) choice of Hamiltonian \hat{H} , jump operators \hat{c}_j and decay rates $\Gamma_j > 0$, such that Eq. (54) is satisfied. The solution to this inverse problem is the subject of Refs. [21, 22], which also proved the existence of a master equation for any arbitrary polynomial f_1 and f_2 .

B. Example: Cubic Liénard system

The application of the ‘quantization’ procedure to the cubic Liénard system (51) is detailed in Refs. [21, 22]. The result is the Lindblad master equation

$$\dot{\rho} = -i[\hat{H}, \rho] + k_0 \mathcal{D}[\hat{a}^\dagger] \rho + \frac{k_2}{2} \mathcal{D}[\hat{a}^\dagger \hat{a} - \hat{a}^{\dagger 2} / 2] \rho + \frac{3k_2}{8} \mathcal{D}[\hat{a}^2] \rho, \quad (56)$$

with the Hamiltonian

$$\hat{H} = \hat{H}_0 + \hat{H}_1, \quad (57)$$

$$\hat{H}_0 = \frac{k_1 + 1}{2} \hat{a}^\dagger \hat{a} + \frac{3k_3}{8} \hat{a}^{\dagger 2} \hat{a}^2 \quad (58)$$

and

$$\hat{H}_1 = \frac{i}{4} [k_0 - i(k_1 - 1)] \hat{a}^2 - \frac{i}{4} \left(\frac{k_2}{2} + ik_3 \right) \hat{a}^\dagger \hat{a}^3 - \frac{i}{16} (k_2 + ik_3) \hat{a}^4 + \text{h.c.}, \quad (59)$$

where h.c. denotes the Hermitian conjugate of all the preceding terms. As stated in the main text, the parameters k_2 and k_3 govern the nonlinear damping and anharmonicity of the oscillator, respectively. This can be seen from the classical equation of motion, or the above quantum master equation. Note that in the quantum case, the parameters $\{k_0, k_1, k_2, k_3\}$ all contribute to the (generalized) squeezing drive denoted by \hat{H}_1 . This gives rise to quantum coherence in the steady state, i.e., off-diagonal elements of ρ in the number basis.

In the main text, it was also stated that the power-law behavior cannot be observed for weak nonlinear dissipation. To see this, suppose k_2 is much smaller than all other parameters. Then, we can make the rotating-wave approximation on the master equation, which yields

$$\begin{aligned}\dot{\rho} &\approx -i[\hat{H}_0 + \hat{H}_1, \rho] + k_0 \mathcal{D}[\hat{a}^\dagger]\rho + \frac{k_2}{2} \mathcal{D}[\hat{a}^\dagger \hat{a}]\rho + \frac{3k_2}{8} \mathcal{D}[\hat{a}^2]\rho, \\ \hat{H}_1 &\approx \frac{i}{4} [k_0 - i(k_1 - 1)] \hat{a}^2 + \frac{k_3}{4} \hat{a}^\dagger \hat{a}^3 + \frac{k_3}{16} \hat{a}^4 + \text{h.c.},\end{aligned}\tag{60}$$

with \hat{H}_0 unchanged. Systematic corrections to the master equation in powers of k_2 can be calculated using the Krylov-Bogoliubov averaging [34].

The approximate master equation (60) is reminiscent of the quantum Stuart-Landau model, studied in Refs. [24, 26, 27, 33] in the context of quantum synchronization. Classically, the Stuart-Landau model describes the behavior of a system near a Hopf bifurcation [23]. In the quantum case (60), the steady state density matrix ρ displays some signatures of a Hopf bifurcation (e.g., the emergence of a quantum limit cycle), but the number distribution vanishes exponentially.